ENTE PER LE NUOVE TECNOLOGIE,
L'ENERGIA E L'AMBIENTE

Serie Innovazione

STORAGE RING FREE ELECTRON LASER, PULSE PROPAGATION EFFECTS AND MICROWAVE TYPE INSTABILITIES

GIUSEPPE DATTOLI, LUCA MEZI, ALBERTO RENIERI

ENEA - Divisione Fisica Applicata
Centro Ricerche Frascati, Roma

MAURO MIGLIORATI

Università degli Studi di Roma "La Sapienza", Rome (Italy)
Dipartimento di Energetica,

RT/INN/2000/24

This report has been prepared and distributed by: Servizio Edizioni Scientifiche - ENEA
Centro Ricerche Frascati, C.P. 65 - 00044 Frascati, Rome, Italy

STORAGE RING FREE ELECTRON LASER, PULSE PROPAGATION EFFECTS AND MICROWAVE TYPE INSTABILITIES

Riassunto

Si sviluppa un modello dinamico per la descrizione dell'evoluzione di un laser ad elettroni liberi in anello di accumulazione con l'inclusione di effetti di propagazione d'impulso e di instabilità a microonda. Si analizzano le condizioni per le quali l'instaurarsi dell'operazione laser può spegnere l'instabilità e si focalizza l'attenzione sulla connessione fra desincronismo della cavità, comportamento pulsato del laser e comportamento instabile del fascio di elettroni: si analizza in particolare l'operazione laser quando il guadagno è prossimo alle perdite della cavità e si osservano effetti particolarmente interessanti.

Abstract

We develop a dynamical model accounting for the storage Ring Free Electron Laser evolution including pulse propagation effects and e-beam instabilities of microwave type. We analyze the general conditions under which the on set of the laser may switch off the instability and focus our attention on the interplay between cavity mismatch, laser pulsed behavior and e-beam instability dynamics. Particular attention is also devoted to the laser operation in near threshold conditions, namely at an intracavity level just enough to counteract the instability, we show that in this region new and interesting effects arises.

Key words: storage ring, FEL, microwave instability, sawtooth

INDEX

STORAGE RING FREE ELECTRON LASER, PULSE PROPAGATION EFFECTS AND MICROWAVE TYPE INSTABILITIES

1 INTRODUCTION

The interplay between the dynamics of laser and of the electron (e-)beam instabilities [1] in Storage Ring (SR) Free Electron Laser (FEL) has been the subject of various investigations and is one of the topics with major interest even though not yet fully understood.

There is a general consensus on the possibility that the on set of the FEL may cure the instability itself, be it transverse or longitudinal.

In the case of instability of microwave nature, the mechanism providing the cure, or better the switching off of the instability itself, traces back to the Boussard criterion [2] and to the FEL induced e-beam energy spread which shifts the threshold of the instability. The combination of the Boussard limit and of FEL mechanisms has allowed the derivation of an intracavity threshold intensity value above which the instability is switched off[3]. The validity of these results has been successively confirmed by means of more sophisticated computations based on fully numerical analyses [4] and therefore the interpretation put forward in Ref. [3,5]appears convincing.

One of the most puzzling experimental evidences has been the fact that in some conditions laser operation can occur without appreciable variation of the e-bunch energy spread and length [6]. This effect, characterizing the near-threshold equilibrium, namely the region in which the FEL has reached a steady or pseudo steady state with an intracavity power just enough to counteract the instability, has been touched on in Ref. [6] and will be more

accurately discussed in the context of the present investigation aimed at clarifying the following points.

a) In the near threshold region may instability and FEL cohabit?
b) Can we identify a regime in which the *switching off* is not definitive and *instability survival may occur*?
c) Can we find near threshold or subthreshold conditions in which the instability is reduced or even switched off without any on set of the laser?
d) How the pulse and slippage effects contribute to the FEL-e-beam instability mutual feedback?

This last point is particularly interesting since the so far developed FEL-instability models do not include pulse propagation effects. We will in particular explore the interplay between FEL and instability in the region of cavity mismatch, where the laser exhibit a pulsed behavior.

The paper consists of two parts, in the first we will combine the 1-D dynamical model developed in ref. 8 in which three coupled non linear differential equations account for the simultaneous evolution of the laser intracavity poser and of the microwave *saw-tooth instability*.

In the second part, we will modify the FEL rate equations to introduce the pulse propagation and slippage effects. Within this last respect, an important role in our analysis will be played by the cavity tuning conditions, which may characterize the laser behavior. When perfect cavity matching is not present, i.e. when the cavity or radiofrequency conditions are such that optical and electron bunches do not exactly overlap, after each round trip, the laser evolution is characterized by a pseudo steady-state, i.e. by a pulsed behavior, when the system has reached saturation. We will, investigate and characterize this regime of operation along with its feedback on the instability evolution.

The equations we will exploit in the first part of the paper are given below

$$\begin{aligned}
\frac{d}{dt}\alpha &= \left[\frac{A}{(1+\sigma^2)^{\frac{1}{4}}} - B(1+\sigma^2)^{\frac{1}{2}}\right]\alpha \\
\frac{d}{dt}\sigma^2 &= \alpha\sigma^2 - \frac{2}{\tau_s}\left(\sigma^2 - x\right), \qquad (1) \\
\frac{d}{dt}x &= Ex\left[\frac{1}{\sqrt{1+\sigma^2}}\frac{1}{1+1.7\mu_\varepsilon(0)^2(1+\sigma^2)} - r\right] + S
\end{aligned}$$

The dynamics of the instability is characterized by α, the parameter accounting for its growth rate and the effect on the energy spread, the laser evolution is described by means of the dimensionless intracavity power x and the induced energy spread. In eq. (1) σ denotes the ratio between the induced and the natural energy spread, r is the ratio between cavity losses and maximum homogeneous FEL small signal gain and $\mu_\varepsilon(0)$ is the energy spread inhomogeneous broadening parameter, associated with the natural e-beam energy spread. The coefficients A,B,E have dimensions s^{-1} and are linked to the accelerator and laser parameters by

$$A = \frac{n}{T_0}\sqrt{\frac{(2\pi)^{3/2} I_0 \upsilon_s \left|\frac{Z_n}{n}\right|}{\left|\frac{E_0}{e}\right|\sigma_{\varepsilon,n}}}$$
$$B = \frac{n}{T_0}(2\pi)\alpha_c\sigma_{\varepsilon,n}\ , \qquad (2)$$
$$E = \frac{0{,}85 g_0}{T_0}$$

where T_0 is the machine revolution period, I_0 the e-beam average current $\left|\frac{Z_n}{n}\right|$ the impedance measured at the n^{th} harmonic of the revolution frequency, $\sigma_{\varepsilon,n}$ is the natural energy spread, ν_s is the synchrotron tune, E_0 the nominal machine energy, α_c the momentum compaction and g_0 the small signal gain coefficient. The coefficient S has dimensions s^{-1} and plays the role of spontaneous emission contribution.

In the forthcoming section we will discuss the system evolution by analyzing the time behavior of the quantities entering in eqs. (2), section 3 will be devoted to the pulse propagation effects and relevant interplay with instability, concluding comments will be presented in section 3

2 FEL DYNMICS AND MICROWAVE INSTABILITY: PRELIMINARY CONSIDERATIONS

The evolution of the saw-tooth instability is shown in Fig. 1, which has been obtained by integrating the first two of eqs. 1, without the inclusion of FEL contributions (x=0). The physical interpretation of this behavior is similar to that of the FEL evolution. The beam

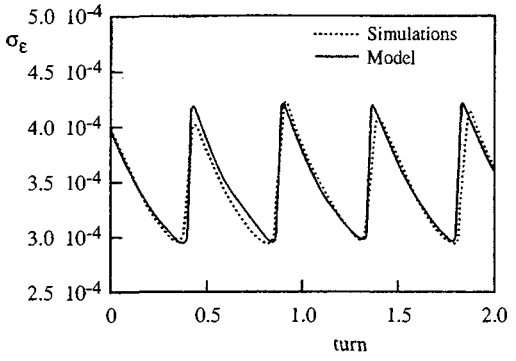

Fig. 1 – Energy spread vs number of turns numerical simulation (dotted line) and model equations (continuous line)

interaction with the ring environment produces the conditions for the instability growth, which is no more supported when the induced energy spread is degraded enough that the gain, associated with α, becomes so small that cannot support the instability growth. When the process stops, the initial energy spread is restored by the damping and the process can start again.

The condition for the switching off of the instability requires that

$$\frac{d}{dt}\alpha = 0, \tag{3}$$

which, owing to the Volterra nature of the equations, describing the saw-tooth evolution, should be regarded such as a pseudo-stationary condition. From the first of eqs. (2) it follows that eq. (3) implies that pseudo-equilibrium is reached whenever the normalized induced energy spread σ reaches the value

$$\sigma^* = \sqrt{\left(\frac{A}{B}\right)^{4/3} - 1} = \sqrt{\left(\frac{I_0}{I_{th}}\right)^{2/3} - 1}\ ,$$

$$I_{th} = \frac{\sqrt{2\pi}\left(\frac{E_0}{e}\right)\sigma_{\varepsilon,\,n}^3\alpha_c^2}{\upsilon_s\left|\frac{Z_n}{n}\right|}\ , \tag{4}$$

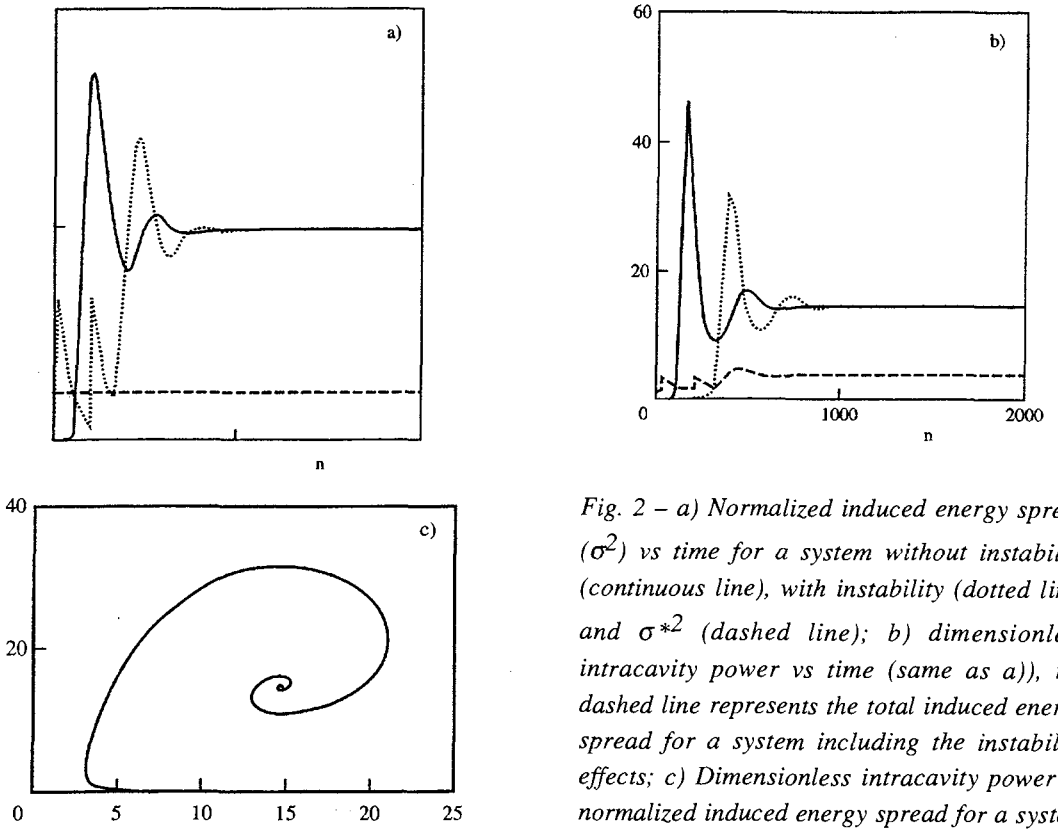

Fig. 2 – a) Normalized induced energy spread (σ^2) vs time for a system without instability (continuous line), with instability (dotted line) and σ^{*2} (dashed line); b) dimensionless intracavity power vs time (same as a)), the dashed line represents the total induced energy spread for a system including the instability effects; c) Dimensionless intracavity power vs normalized induced energy spread for a system affected by instability. $A=9\times10^4$, $B=3\times10^4$, $E=10^4$, $\mu_\varepsilon(0)=0,1$, $r=0,2$.

where I_{th} is the Boussard threshold current, above which the instability should manifest itself. We will use σ^* as a reference threshold value for the FEL induced energy spread above which the instability, if present, is switched off.

The parameters A and B play a role of paramount importance, they fix indeed the amplitude and the period of the pseudo oscillations of the energy spread due to the instability. Being the eqs. (2) non linear, the dynamics of the system will be dependent on the choice of the initial conditions of α_0,σ_0. This point is particularly important and its consequence will become clear in the forthcoming analysis. The parameters E and r control the dynamics of the intracavity laser intensity, the FEL-instability feedback occurs through the induced energy spread to which both contribute.

The so far developed considerations suggest that FEL and sawtooth dynamics may be viewed as competing mechanisms, which are both inducing an energy spread, which is the parameter controlling the growth of both signals.

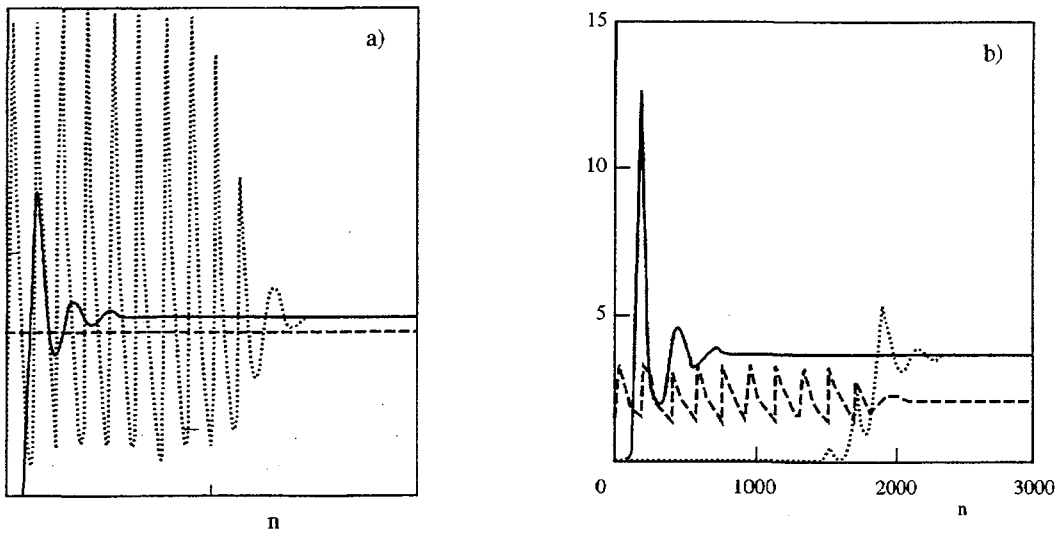

Fig. 3 – Same as fig. 1 r=0.43

In figure 2 we have reported the system evolution vs time (each time step corresponds to 2.4×10^{-2} ms) for $A=9\times10^4$ s^{-1}, $B=3\times10^4$ s^{-1}, $E=10^4$ s^{-1}, $S=0$, $\alpha_0=\sigma_0=1$ and $r=0.2$ with this choice of parameters the FEL induced energy spread is well above the threshold value σ^* and the laser, apart from a slight initial lethargy, reaches a stable final configuration as shown in the stability diagram of fig. 1c. It is worth stressing that the initial noise due to the instability is cancelled by the on set of the FEL which reaches the same stationary value it would reach in absence of the instability.

A better idea is given in figs. 3, the same as figs 2 for $r=0.43$, in this case the induced energy spread is just above σ^* and the system takes a longer time to reach the stable configuration it would achieve in absence of instability.

Figures 4 is more interesting, the induced energy spread at $r=0.45$ is very close to σ^* the laser seems to be switched on and is able to counteract the instability, notwithstanding the laser is no more supported by sufficient gain and the system reaches a stationary configuration (see Fig. 4b) decaying with the decay time of the cavity. We must underline that the instability is not really switched off, the stability growth rate α does not reach exactly the value zero, as it happens in the case in which the induced energy spread is above the threshold value (see figs 5 where we report α vs time for two different values of r).

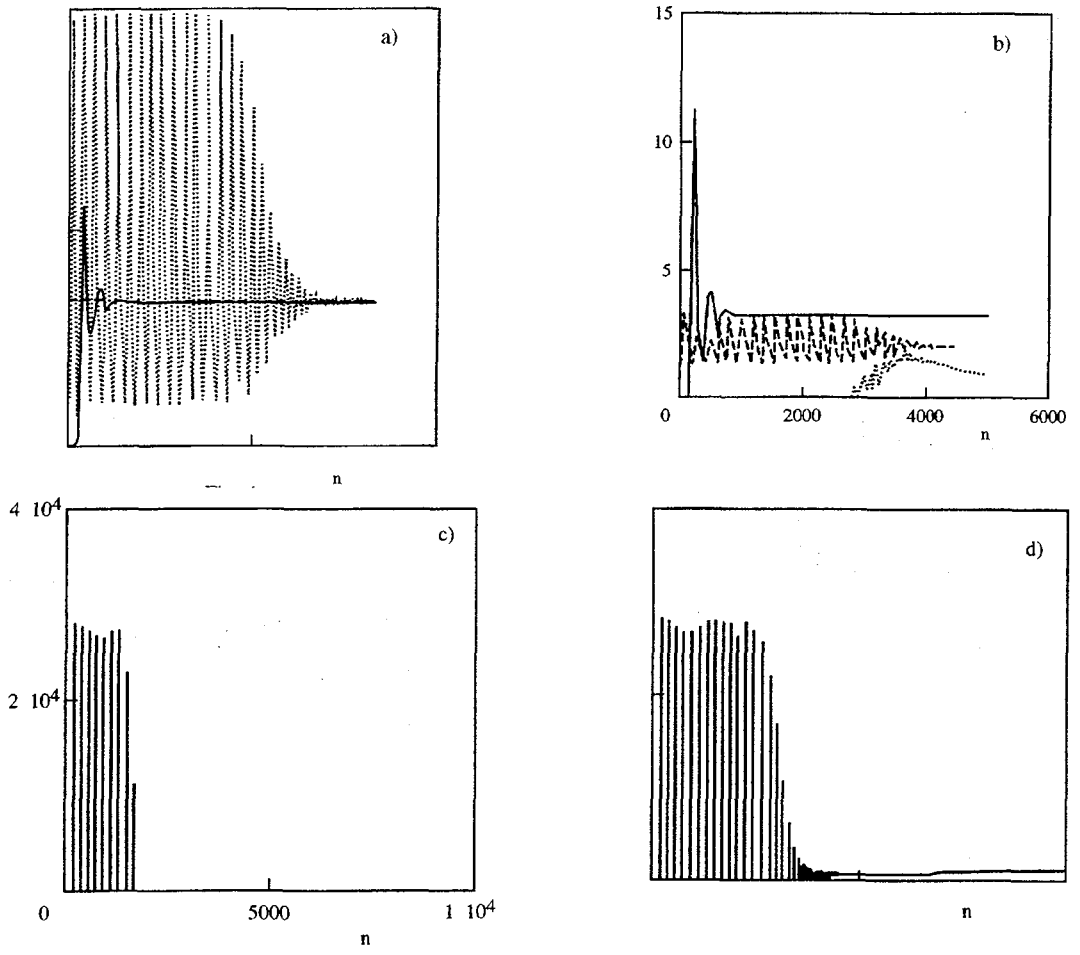

Fig. 4 – Same as fig. 1 r=0.45

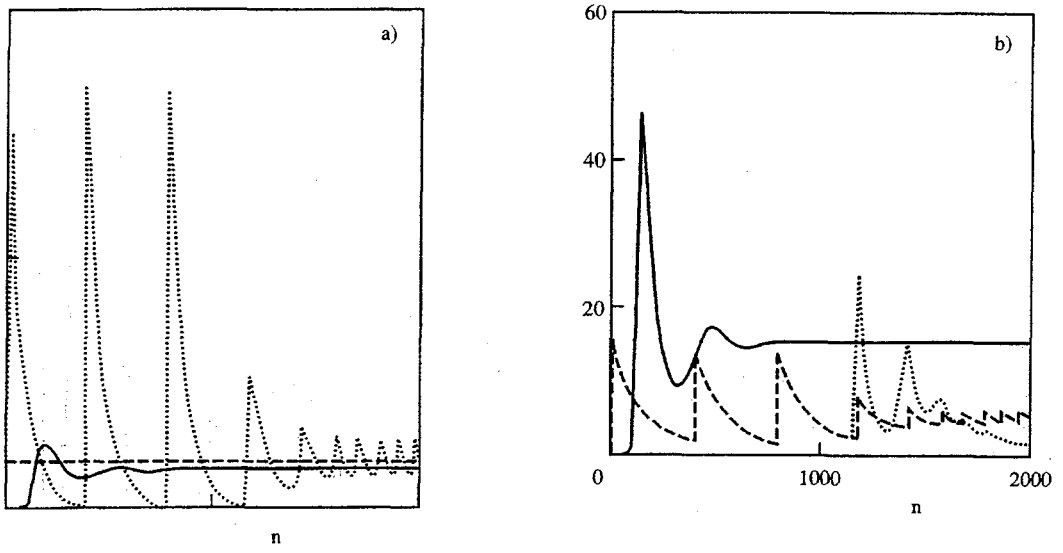

Fig. 5 – Instability growth rate α vs time: a) r=0.43, b) r=0.45

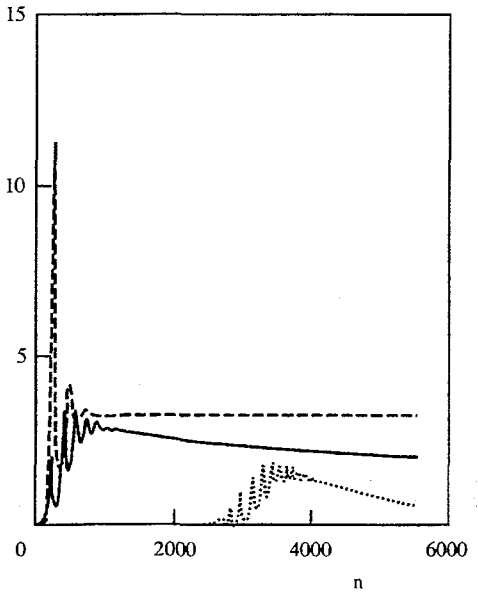

Fig. 6 – Same as fig. 4b) with the inclusion of the spontaneous contributions, modeled with a random fluctuation contribution of amplitude S~90

In Fig. 6 we show the effect on the evolution of a non-vanishing spontaneous emission term, we have considered a case in which the effect should be more significant, namely the situation of fig. 4. It is evident that the presence of the new term does not modify the system evolution in a significant way.

3 INSTABILITY AND PULSE PROPAGATION EFFECTS

In the previous section we have discussed the FEL-S.R. Instability interplay, without the inclusion of effects due to the finite longitudinal e-bunch structure and to cavity mismatch effects, which may provide a lack of overlapping between electron and photon bunches, after each cavity round trip. This effect has been shown to provide a pulsed behavior of the laser operation when the system is close to saturation. It is therefore worth to investigate the combination of cavity mismatch induced pulsed behavior and the saw-tooth contributions. Before entering into the specific aspects of the problem we will discuss the physical origin of the mechanisms leading to the pulsed laser evolution.

The equations we will use to model the problem dynamics are given below

$$\begin{aligned}
&\frac{d}{dt}\alpha = \left[\frac{A}{(1+\sigma^2)^{1/4}} - B(1+\sigma^2)^{1/2}\right]\alpha \ , \\
&\frac{d}{dt}\sigma^2 = \alpha\sigma^2 - \frac{2}{\tau_s}\left(\sigma^2 - \bar{x}\right) \ , \\
&\frac{d}{dt}x(\tau,t) = E\left[x(\tau+\delta,t)G(\tau,\sigma) - \bar{r}x(\tau,t)\right] + S(\tau), \quad \bar{r} = \frac{\eta}{g_0}
\end{aligned} \tag{5}$$

where

$$\begin{aligned}
&G(\tau,\sigma) = \frac{2\pi}{\sqrt{1+\sigma^2}}\int_0^1 d\xi(1-\xi)\sin(\upsilon\xi)e^{-\frac{(\pi\mu\varepsilon\xi)^2}{2}(1+\sigma^2)}e^{-\frac{\tau^2}{2(1+\sigma^2)}} \\
&\bar{x} = \int_{-\infty}^{\infty} x(\tau,t)d\tau, \quad \tau = \frac{z}{\sigma_z} \ ,
\end{aligned} \tag{6}$$

where τ is the longitudinal coordinate normalized to the e-bunch length. The function $G(\tau,t)$ denotes the gain function including the line shape (υ is the frequency detuning parameter), and the e-bunch longitudinal distribution, which is assumed a gaussian at any time. The term accounting for the increase of the energy spread and bunch lengthening is accounted for by the $(1+\sigma^2)$ contributions. The factor δ specifies the amount of mismatch of the peak of the optical pulse distribution with respect to that of the e-bunch.

In figs. 7-10 we have summarized the results of the numerical integration of our model equations. The case δ=0 does not provide any significant differences with respect to the dynamics discussed in the previous section, apart from an initial transient the optical pulse is stable during all the system evolution which is finally characterized by a steady state operation.

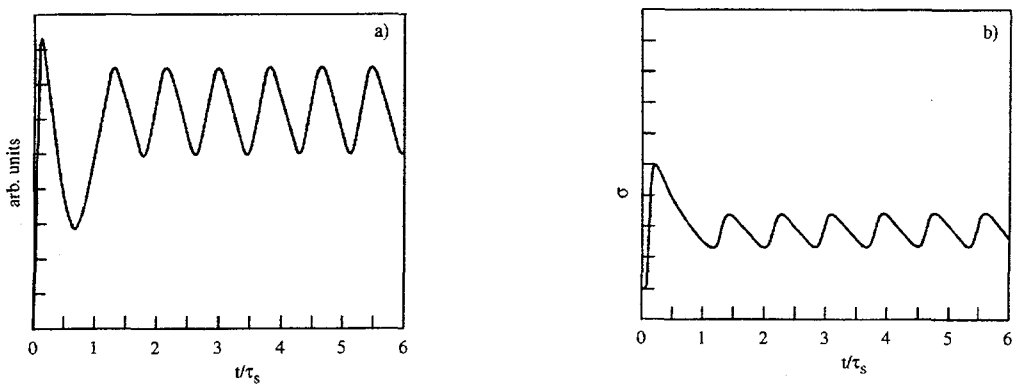

Fig. 7 – a) evolution of the optical packet intensity $\bar{x}$; b) evolution of the e-beam induced energy spread and for g_0=5%, η=1%, τ_s=1.5×10^{-3}s, T_0=2×10^{-7}s, δ=0.1 with a spontaneous emission contribution S~5, and without instability effects.

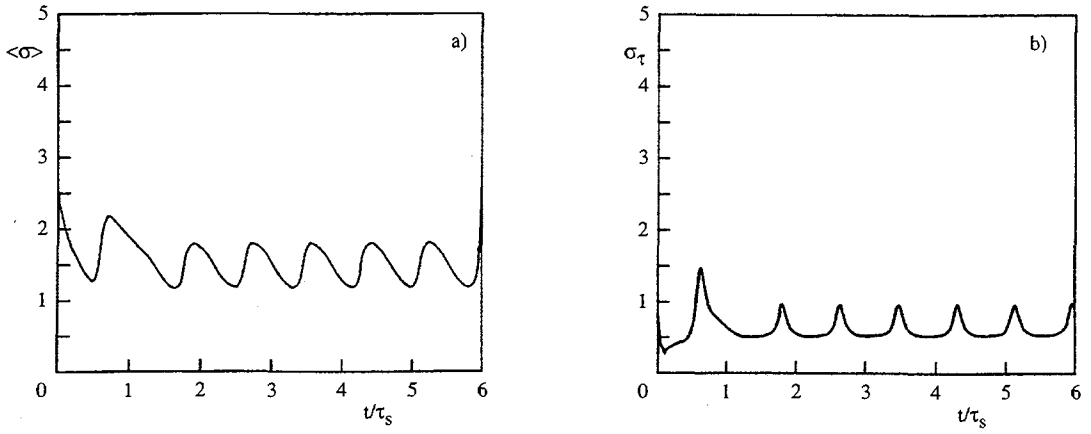

Fig. 8 – a) Evolution of the optical packet centroid, b) Evolution of the r.m.s. of the optical packet same parameters of Fig. 7

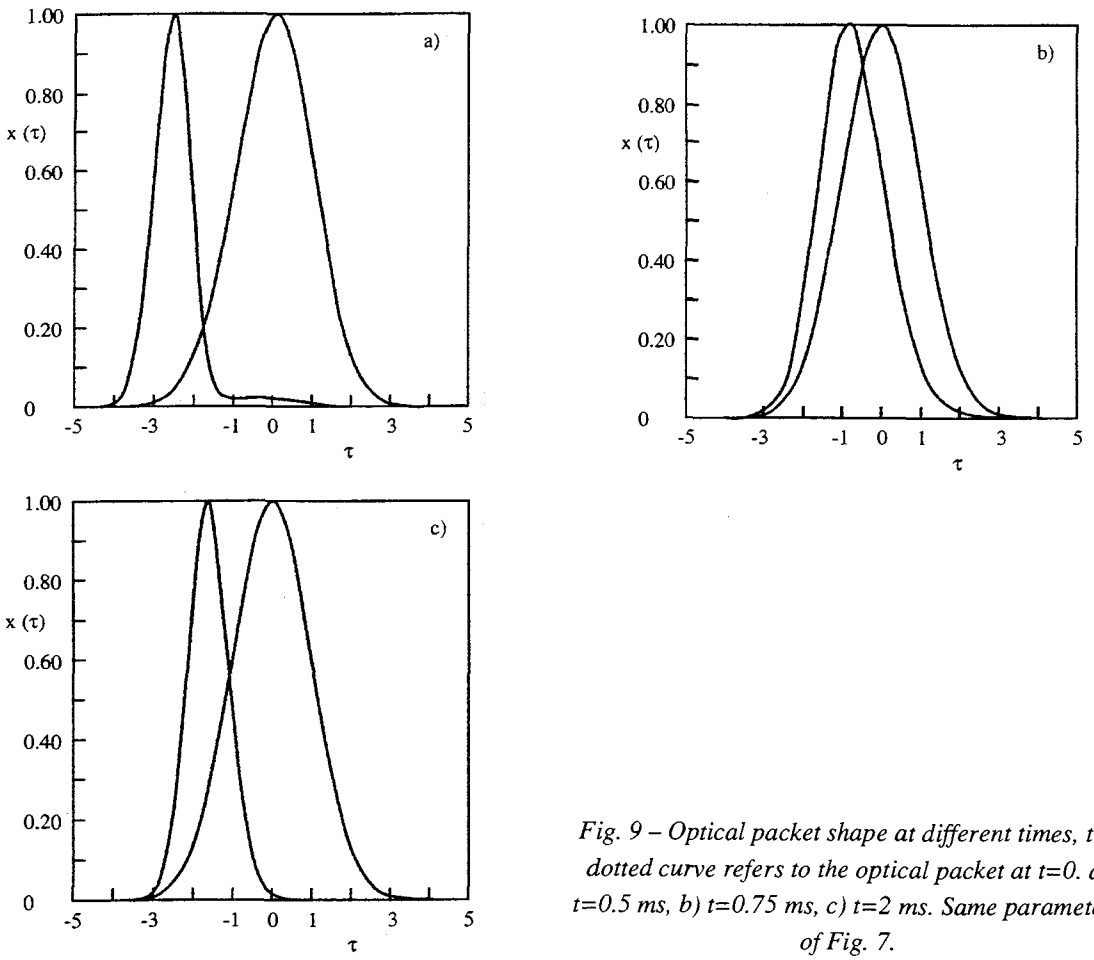

Fig. 9 – Optical packet shape at different times, the dotted curve refers to the optical packet at t=0. a) t=0.5 ms, b) t=0.75 ms, c) t=2 ms. Same parameters of Fig. 7.

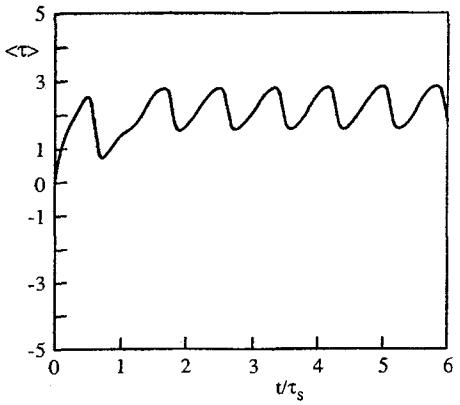

Fig. 10 – Evolution of the optical packet centroid same parameters of fig. 7 and δ=-0.1

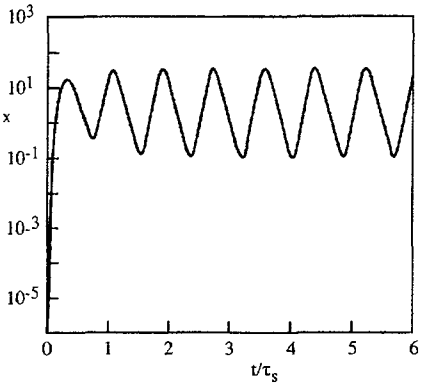

Fig. 11 – Same as fig. 7 with the inclusion of instability effects $A=9\times10^4$, $B=3.5\times10^4$, $\alpha(0)=1$, $\sigma(0)=1$

The situation is different for $\delta\neq0$, as shown in fig. 7 relevant to the case $\delta=0.1$. As already remarked the system does not reach a real steady state operation, as indicated by figs 7a,b accounting for the optical dimensionless intensity and σ respectively. To give an idea of the optical packet dynamics we have reported in figs 8a,b the evolution of the first and second moments of the optical packet distribution. The figures suggest that the optical packet breath and its center moves back and forth. Initially the packet moves back, experiences less gain and tends to be reduced in amplitude, then when it has reached a minimum it moves towards the beam center and increases its amplitude. Once it has reached the maximum amplitude the process start again, in figs 9 we report the bunch at different times. We must underline that for negative δ value (optical bunches ahead the electron beam) the situation is exactly specular, see e.g. Fig. 10 where we have reported (τ). In the case in which we include the contributions from the saw-tooth instability the situation does not change in a significant way. It may happen that in the case of perfect matching the system has enough gain to overcome the instability and to reach a stable operation, but in the mismatched region the gain is not sufficient so the laser does not even start. It may happen that the system has sufficient gain to develop also for mismatched configurations. In this case the system dynamics is described by figs 11, if the laser start the instability is counteracted and if so the packet dynamics is more or less the same as in the case without instability, with the only effect that the longitudinal excursion is less wide.

In the following we will present further comments on the result of this section.

4 CONCLUDING REMARKS

The results so far obtained suggests that

a) the FEL is able to counteract the instability when the induced energy spread is larger than the threshold value fixed by eq. (3)

b) if above threshold, the equilibrium laser power is that the system would reach in absence of the instability

c) the FEL and the saw tooth instability cannot cohabit

d) In near-threshold conditions (just above threshold) the FEL may operate without any appreciable increase of the energy spread and bunch lengthening

e) In some subthreshold conditions the laser may be excited but, since it is not adequately supported by the system gain, the intracavity intensity decays with the cavity depletion time.

f) when pulse propagation effects are included no significant variations with respect to the above points emerge, except that in the presence of instability FEL operation is not ensured in the cavity mismatch region if the gain is not sufficient.

This point e) is better illustrated by figs 12 where we have reported the analogous of figs (2-4)

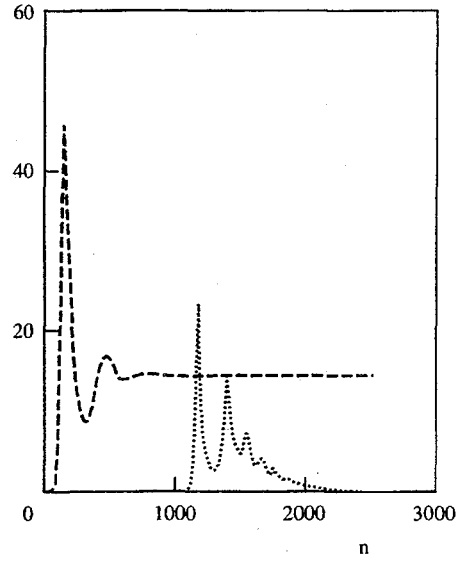

Fig. 12 – Dimensionless intracavity power vs time for $A=9\times10^4$, $B=10^4$, $2/\tau_s=600$ $r=0.2$, without instability (dashed line) with instability (dotted line)

for $A=9\times10^4$, $B=10^4$, $E=10^4$, $\frac{2}{\tau_s}=600$ and r=0.2. The amplitude and the period of the instability induced pseudo oscillations of the normalized energy spread are significantly larger than before, the FEL induced energy spread is less than the threshold value, the system try to lase at the bottom of an energy spread pseudo oscillation and then it lasts for some time and then decays. It is important to emphasize that even though the laser cavity is depleted the instability is partially cured, the associated fluctuations are indeed significantly reduced.

The FEL near threshold operation exhibits a fairly interesting behavior, it is indeed very unstable and the laser gain may be characterized by a non linear dependence on the current.

By recalling that above the Boussard current threshold either the bunch length and energy spread exhibit a current dependence of the type $I^{1/3}$, we can write the FEL maximum gain as

$$G^* = 0,85 g_0 \frac{\left(\frac{I}{I_{th}}\right)^{2/3}}{1+1.7\mu_\varepsilon(0)^2\left(\frac{I}{I_{th}}\right)^{2/3}} \tag{7}$$

where g_0 is the threshold current small signal gain coefficient. It is evident that a deviation from the linear dependence may be the signature that the system may operate close to the instability threshold. Other effects, like the potential well distortion, discussed in ref. (5), may lead to a similar dependence, but they do not affect the system dynamics according to the interesting phenomenology discussed in this paper and produce a mere gain reduction with respect to the natural case.

Before closing the paper there are other points worth to be discussed

1) We have noted that it may happen that both the laser and the instability are switched off. This fact may sound strange and one may argument against that the system should be restored to the original situation by damping, this true in the linear regime the equations governing the instability are strongly non linear and dependent on the initial conditions. The interaction with the FEL create different operating conditions which may completely modify the system dynamics.

2) We have noted that in the mismatched region the optical packet dynamics is characterized by the peculiar behavior in which the packet moves back and forth with respect to the e-bunch center the amplitude of the oscillations can be understood from fig. (8), where we have reported the optical packet centroid position in unit of σ_z. It is evident that $\bar{z}\sim\sigma_z$, by assuming that σ_z is of the order of few cm, we can infer that the amplitude of the centroid

oscillations be of the order of hundreds of ps. Such a result is in agreement with the experimental data from Super Aco 6. The same conclusion holds for the optical packet dispersion.

The physical reasons underlying the previously described behavior can be understood by inspecting the third of eqs. (5), which, for small δ values and around the peak of the bunch current distribution, can be written as

$$\frac{\partial}{\partial t}x(\tau,t)=E\left[\frac{G_1\left(\upsilon,\mu_\varepsilon\sqrt{(1+\sigma^2}\right)}{\sqrt{1+\sigma^2}}\left(x+\delta\frac{\partial x}{\partial\tau}+\frac{\delta^2}{2}\frac{\partial^2 x}{\partial\tau^2}-\frac{1}{2}\frac{\tau^2}{1+\sigma^2}\right)-\bar{r}x(\tau,t)\right]+S(\tau) \qquad (8)$$

where $G_1(\upsilon,\mu_\varepsilon)$ is the FEL gain including the inhomogeneous energy spread contribution. The structure of eq. 8 is that of a Fokker-Plank equation with a quadratic potential. The term with the first derivative accounts for the optical packet shift, the term with the second derivative is responsible for the diffusive part and the potential-contribution is repulsive.

Even though the model is capable of reproducing the system dynamics, further improvements are necessary, we believe that the complete symmetry between positive and negative δ values in an artifact of the model equations which can be eliminated by working with the full pulse propagation equation as it will be discussed in a forthcoming investigation.

ACKNOWLEDGMENTS

The authors express their sincere appreciation to Prof. L. Palumbo for enlightening discussions on the physics of S.R. Instabilities, interesting and and stimulating discussions with M. Billardon and V. Litvinenko are sincerely recognized. This work has been partially supported by European contract ERB 4061 PL 97-0102.

REFERENCES

[1] See the proceedings of the workshop "Non linear problems in Charged Beam Transport in Linear and Recirculated Accelerators" Frascati 13-15 May 1998 published in N. Cimento 112A, n. 5 may (1999) ed. by Dattoli.

[2] G. Dattoli, L. Mezi, M. Migliorati and A. Renieri *Free Electron Laser and Storage ring Microwave Instability*, Proc. of EPAC 1998, Stockholm, June 22-26 (IOP publishing Bristol) p. 673, 1998

[3] D. Boussard, CERN LABII/75-2 (1975)

A. Chao, *Physics of collective beam instabilities in high energy accelerators*, (J. Wiley and sons, New York) 1993

[4] G. Dattoli, L. Mezi, M. Migliorati, L. Palumbo and A. Renieri, Nucl. Instrum. & Meth. A433, 683 (1999)

M. Migliorati, L. Palumbo, G. Dattoli and L. Mezi, Nucl. Instrum. & Meth. A437, 134 (1999)

[5] G. Dattoli, L. Mezi, M. Migliorati and A. Renieri, Eur. Phys. J. D6,375 (1999)

[6] See e.g. D. Nutarelli "Dynamique et Performaces du laser à electrons libres de Super-ACO avec une cavité RF Harmonique à 500 MHz" These Universitè de Paris-sud U.F.R. Scientifique d'Orsay Janyary 20, 2000

Edito dall' ENEA
Unità Comunicazione e Informazione
Lungotevere Grande Ammiraglio Thaon di Revel, 76 - 00196 Roma
Sito Web http://www.enea.it

Stampa Laboratorio Tecnografico - C.R. Frascati
Finito di stampare nel mese di gennaio 2001